Highlights

- A dual impedimetric aptamer-based platform directly deployed in diluted serum samples.
- Combination of two aptamers recognizing different regions of PSA.
- The platform provides as output a glycan PSA score.
- The glycan score discriminates prostate cancer from other benign diseases.

A. Díaz-Fernández, R. Miranda-Castro, N. de-los-Santos Álvarez, M.J. Lobo-Castañón, P. Estrela
Impedimetric aptamer-based Glycan score for discrimination of prostate cancer form other prostate diseases
Biosensors and Bioelectronics 175 (2021) 112872

Graphical Abstract

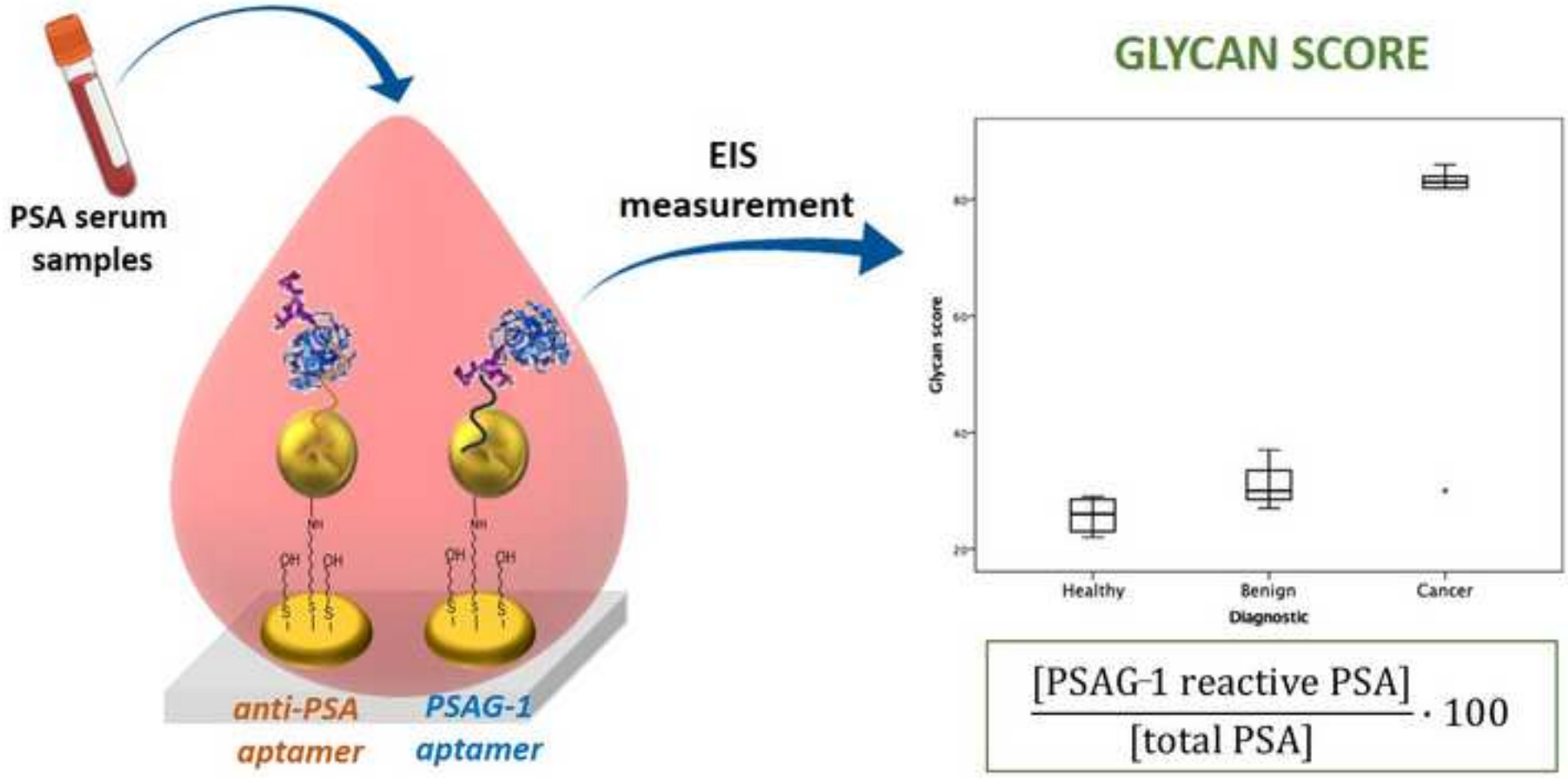

Impedimetric Aptamer-based Glycan PSA Score for Discrimination of Prostate Cancer from other Prostate Diseases

Ana Díaz-Fernández[1,2], Rebeca Miranda-Castro[1,2], Noemí de-los-Santos-Álvarez[1,2], María Jesús Lobo-Castañón[1,2]* and Pedro Estrela[3,4]*.

[1] Departamento de Química Física y Analítica. Universidad de Oviedo, Av. Julián Clavería 8, 33006 Oviedo, Spain.

[2] Instituto de Investigación Sanitaria del Principado de Asturias, Avenida de Roma, 33011 Oviedo, Spain.

[3] Centre for Biosensors, Bioelectronics and Biodevices (C3Bio), University of Bath, BA2 7AY, Bath, United Kingdom.

[4] Department of Electronic and Electrical Engineering, University of Bath, BA2 7AY, Bath, United Kingdom.

* Corresponding author:

MJLC: mjlc@uniovi.es

PE: p.estrela@bath.ac.uk

Abstract

Prostate specific antigen (PSA) is the common biomarker for prostate cancer (PCa). However, its lack of specificity to differentiate PCa from benign prostate disorders stimulates the search for alternative cancer biomarkers to improve the clinical management of the patients. Different studies have described changes in the core-fucosylation level of PSA between PCa patients and healthy controls. To exploit these findings, we have adapted an impedimetric aptamer-based sensor to the dual recognition of PSA. Two different aptamers, PSAG-1 and anti-PSA, are immobilized onto two adjacent nanostructured gold electrodes. The direct binding from diluted serum samples of specific glycosylated-PSA to the first sensor and total PSA to the second one leads to changes in the charge transfer resistance, which correlate to the amount of glycosylated and total PSA in the sample. The sensors are able to measure PSA in serum with a dynamic range between 0.26 and 62.5 ng/mL (PSAG-1) and from 0.64 to 62.5 ng/mL (anti-PSA), with a reproducibility of 5.4 %. The final output of the proposed platform is the ratio between PSAG-1 reactive PSA and total PSA, defined as the glycan score. The glycan score was tested in serum samples from patients with different pathologies, showing excellent correlation between the measured score and the known diagnosis of the patients. Hence this dual aptamer-based impedimetric biosensor could be used as a minimally invasive method for the diagnosis of prostate cancer.

Keywords: Aptasensor; Glycosylation pattern; Impedimetric sensor; Prostate cancer; PSA

1. Introduction

Prostate cancer (PCa), the most common solid tumor in men (Butler et al., 2020), is usually suspected on the basis of a digital rectal exam and elevated serum prostate-specific antigen (PSA) levels. However, PSA is an organ specific but not cancer-specific biomarker. In consequence, serum PSA test has limited diagnostic value, with a high false positive rate as confirmed after histopathological verification of prostate biopsy (Schröder et al., 2009). This leads to many unnecessary repeated prostate biopsies, with the associated risks and overtreatment of clinically insignificant cancers (Lomas and Ahmed, 2020; Macefield et al., 2010). Therefore, significant effort has been focused on the development of new methods able to improve the diagnostic performance of PCa, especially for patients with serum PSA levels in the range 4-10 ng/mL, the ambiguous area called the diagnostic grey zone (Saini, 2016).

Besides PSA, the US Food and Drug Administration (FDA) has recently approved a few new tests such as the prostate health index, which combines the detection of different molecular forms of PSA in serum (Catalona et al., 2011) and PCA3 score, a ratio between the concentration of prostate cancer gene 3 (PCA3) and PSA mRNA molecules in first-catch urine after a post-digital rectal exam (Jung et al., 2004). Many other biomarkers remain at the investigation or validation phase (Saini, 2016). Among them are altered PSA glycosylation patterns, which are potentially useful in the development of more reliable diagnostic tools for PCa (Gilgunn et al., 2013).

Glycosylation is a post-translational modification that has been shown to play important roles in development and progression of cancer. There are numerous studies linking changes in the glycan composition of PSA to malignant transformation and prostate tumor progression (Munkley et al., 2016). PSA contains N-glycans attached to

the amine nitrogen of asparagine 69 (Asn_{69}). These are sugars extremely structurally diverse, but all contain a saccharide core with a N-acetylglucosamine (GlcNAc) directly linked to the Asn_{69}. Fucosylation of this GlcNAc in the core of the N-glycans (core-fucosylation) is significantly altered in patients with PCa (Peracaula et al., 2003; Song et al., 2015). Despite this, the study of specific glycoforms of PSA has lagged behind because there is still no single test for measuring the percentage of PSA with tumor-specific glycan moieties. This information is typically obtained by combining an ELISA for measuring total or free PSA and lectin immunosorbent assays for detecting specific glycosylated forms of PSA (Jolly et al., 2016; Li et al., 2015; Llop et al., 2016; Pihíková et al., 2016a, 2016b; Xia et al., 2017).

In response to the need for improved tests for PCa diagnosis, we have recently developed an aptamer (PSAG-1) targeting the glycosylation site of PSA (Díaz-Fernández et al., 2020). There are other RNA (Jeong et al., 2010; Svobodova et al., 2013) and DNA-aptamers (Díaz-Fernández et al., 2019; Li et al., 2018; Park et al., 2016; Savory et al., 2010) recognizing PSA, but PSAG-1 is the only one that achieves the binary recognition of this glycoprotein through both the peptide region and the innermost sugar residues, in the core region of the protein. Given the above attributes, we were motivated to include this aptamer in an impedimetric label-free aptasensor (Jolly et al., 2017) for the sensitive measurement of a specific fraction of PSA in serum samples. When compared with other aptamer-based sensors (Akiba and Anzai, 2016; Damborska et al., 2017; Daniel et al., 2013; Ghorbani et al., 2019; Negahdary et al., 2020; Srivastava et al., 2018), this is a simple approach where the target-recognizing aptamer is immobilized by one end to a nanostructured gold electrode. The direct binding of the protein alters the charge-transfer resistance when the sensor is electrochemically interrogated in the presence of a redox probe. Using this approach, we

describe here a platform for the convenient measurement of an empirical index, a glycan score, in serum samples. The platform uses a dual receptor approach, combining two different aptamers: anti-PSA (Savory et al., 2010) recognizing total PSA and PSAG-1 (Díaz-Fernández et al., 2020) that binds to core-fucosylated PSA. The percentage of PSAG-1 reactive PSA is shown to be a more accurate index than total PSA for the diagnosis of PCa.

2. Materials and methods

2.1 Materials

The DNA aptamers anti-PSA: AATTAAAGCTCGCCATCAAATAGCTTT and PSAG-1: GAGCGGGGTTGCTGGGATGATAAGGCCCCTTTGATGTCTG were obtained from Metabion (Germany) as lyophilized powder after HPLC purification. Both aptamers were synthesized with a thiol group at the 5' end and a spacer of six carbons and five thymine bases. PSA Certified Reference Material BCR®-613 and albumin from human serum were purchased from Sigma-Aldrich (Spain and UK). Recombinant Human PSA (ab126692) from *Escherichia coli* and Recombinant Human Lipocalin-2, NGAL, from HEK 293 cells (ab167728) were obtained from Abcam (UK). 11-Amino-1-undecanothiol hydrochloride, phosphate buffer saline (PBS) tablets, phosphate buffer and potassium chloride were purchased from Sigma-Aldrich (Spain and UK) as molecular biology grade reagents. 6-Mercapto-1-hexanol (MCH), gold nanoparticles (20 nm diameter, stabilized), potassium hexacyanoferrate (III), potassium hexacyanoferrate (II), hydrogen peroxide 30%, ammonium hydroxide 20% and acetone were also supplied by Sigma-Aldrich (Spain and UK). Absolute ethanol was purchased from VWR (Spain). Sulfuric acid (95-98 %) was supplied by J.T. Baker (Fisher Scientifics, Spain). Microscope slides with round edges were obtained from VWR

(UK). All aqueous solutions were prepared using ultra-pure water from a MilliQ system (Millipore).

2.2 PSA serum samples

Serum samples from twelve men as well as a pool of women serum samples were provided by the clinical analysis laboratory at Hospital Universitario de Cabueñes (Gijón, Spain). Male serum samples were obtained from patients with elevated PSA levels (> 4 ng/mL), with a final diagnosis confirmed by prostate biopsies. The female serum sample was used as PSA negative control.

2.3 Instruments

Electrochemical measurements were performed in a μAutolab III/FRA2 and Autolab Pgstat-12 with FRA2 module for impedance measurements connected to a computer with NOVA 2.1 software (Metrohm, The Netherlands). For all the electrochemical measurements an external Ag|AgCl reference and Pt counter electrodes were used. Electrochemical impedance spectroscopy (EIS) measurements were performed in a solution of 5 mM $[Fe(CN)_6]^{3-}$ and 5 mM $[Fe(CN)_6]^{4-}$ in 1× PBS at 0.22 V vs Ag|AgCl, the formal potential of the redox couple as measured by cyclic voltammetry. The frequency was varied in the range from 100 kHz to 100 mHz with an amplitude of 0.01 V.

Surface plasmon resonance (SPR) measurements were carried out using an Autolab ESPRIT SPR instrument (Metrohm, The Netherlands) equipped with a two-channel cuvette and an autosampler, which is controlled by Data Acquisition Software (version 4.4). The temperature of the cell was controlled with a thermostat HaakeD1 (Germany). The SPR gold sensors were obtained from XanTec bioanalytics (Germany).

2.4 SPR measurements

SPR gold chips were cleaned with piranha solution (70 % H_2SO_4+ 30 % H_2O_2) for 2 min and then washed with water and ethanol and dried with nitrogen. A mixed self-assembled monolayer of the thiolated aptamer and MCH was formed onto the surface of the chip. The surface was incubated at 4 °C overnight with a mixture of aptamer and MCH in a 1:100 ratio, with a total thiol concentration of 100 µM in PBS. Then the surface was cleaned with PBS and dried with nitrogen before placing it onto a clean hemi-cylinder prism, previously coated with a drop of immersion oil. Finally, the surface was blocked with 50 µL of 1 mM MCH in PBS for 1 hour at 25 °C.

To measure the binding of PSA to the surface, baselines in both channels were acquired by triplicate injections of PBS buffer for 5 min each. Then the association step was performed adding increasing concentrations of PSA in one channel and buffer or NGAL in the reference channel for 10 min. After washing the surface with PBS, the dissociation step was registered for 10 min to eliminate the unspecifically bound molecules and a stable signal was obtained. The difference between the signal after the dissociation step and the baseline before the interaction is related to the binding of the protein to the aptamer after subtraction of both the buffer and the non-specific signal measured in the reference channel. After that, a new cycle was performed with the next PSA concentration without regeneration. All the injections and signals registered were performed automatically by the ESPRIT autosampler and sequencer. During each injection the solution was continuously stirred, and all the interactions were thermostated at 25 ± 1 ˚C.

2.5 Fabrication of evaporated gold electrodes.

The working gold electrodes were prepared in-house by thermal evaporation on glass slides. The slides were first cleaned by immersion in a solution of $H_2O/NH_4OH/H_2O_2$ 5:1:1 for 30 minutes. Then they were rinsed sequentially with acetone, isopropanol and

water and dried with nitrogen. Finally, they were cleaned with oxygen plasma (Diener Plasma Chamber with Oxygen, Zepto, Germany) at a pressure of 0.2 mbar and a voltage of 10 mV for 10 minutes.

Chrome and gold pieces with a size of 1-3 mm were cleaned with acetone and isopropanol before thermal evaporation and deposition on a glass slide with a mask to define the shape of the working electrode (a circle with 4 mm of diameter). An adhesion layer of 10 nm chromium and 100 nm of gold were subsequently evaporated using a BOC Edwards (USA) thermal evaporator. Evaporated gold electrodes were cleaned prior to their use with acetone vapour for 4-5 times and with UV-ozone for 15 min.

2.6 Aptasensor fabrication

The impedimetric sensors were fabricated using a previously established approach (Jolly et al., 2017), schematically shown in **Figure 1A**. First the gold electrodes were nanostructured with gold-nanoparticles (AuNPs). With this aim, a self-assembled monolayer (SAM) of 11-amino-1-undecanothiol was formed by overnight incubation at 4 °C on the evaporated gold electrodes in 50 µL of 1 mM 11-amino-1-undecanothiol in pure ethanol. Following this, the electrode surface was rinsed with ethanol and dried with nitrogen. Then the surface was blocked with 1 mM MCH in ethanol for 1 hour at RT. Next, the electrodes were washed with ethanol and water and dried with nitrogen. Thereafter they were incubated overnight at RT with 50 µL of the commercial AuNPs solution. Onto the new gold surface, a second mixed SAM was formed by incubation with a solution 1:100 of the thiolated aptamer (anti-PSA or PSAG-1) and MCH in PBS buffer (PBS 1 × + 2.7 mM KCl, pH 7.4) for 2 hours at RT. The total concentration of thiols in the solution was 100 µM. Then the electrodes were rinsed with PBS buffer and incubated with this buffer for 3 hours to stabilize the SAM prior to the EIS measurements.

2.7 PSA detection

PSA solutions were prepared by serial dilution of the stock PSA standard in PBS buffer or serum diluted 1:5. For PSA detection, 50 µL of each solution was incubated onto the modified working electrode for 30 min at room temperature. Then the electrodes were rinsed with PBS and the impedance spectrum was recorded.

3. Results and discussion

We employed a DNA aptamer (PSAG-1) previously developed in our group, which displays high affinity and selectivity towards PSA, recognizing both the peptide region surrounding the glycosylation site and the glycan at the core, including fucose (Díaz-Fernández et al., 2020). Because tumour transformations imply changes in the N-glycan moiety attached to PSA, and specifically in the level of core-fucosylation, we investigated the use of a dual impedimetric platform for obtaining information about the fraction of serum PSA that is PSAG-1 reactive, and its utility as an indicator of PCa. This requires a second aptamer capable of entrapping the total serum PSA, denoted as anti-PSA (Savory et al., 2010). Both aptamers are immobilized onto nanostructured gold electrodes through a thiol group (**Figure 1A**). The gold nanoparticles are attached to the evaporated gold surface through the interaction with an amine-terminated self-assembled monolayer of 11-amino-1-undecanothiol, and MCH acts as backfiller to prevent non-specific interactions. The increase in the active area allowed an effective immobilization of the aptamer in a subsequent step, using MCH as diluent.

Electrochemical impedance spectroscopy (EIS) allowed us to monitor the different steps of the fabrication process (**Figure 1B**). The charge transfer resistance, R_{ct}, of the bare gold electrode (759 ± 20 Ω) decreased after the first monolayer formation (117 ± 19 Ω), which is due to the positive charges of the amino groups electrostatically attracting the redox probe in solution. The coating with AuNPs led to an increase in the R_{ct} value (420

± 47 Ω), a value that is still lower than the initial resistance for the bare gold, demonstrating the benefits of creating a nanostructured gold surface with improved electron transfer properties and increased surface area for subsequent modification. Finally, after the aptamer immobilization we observed an increase in R_{ct} (2864 ± 155 Ω) due to the electrostatic repulsion by the negatively charged oligonucleotide. These results suggest a correct fabrication of the aptasensor.

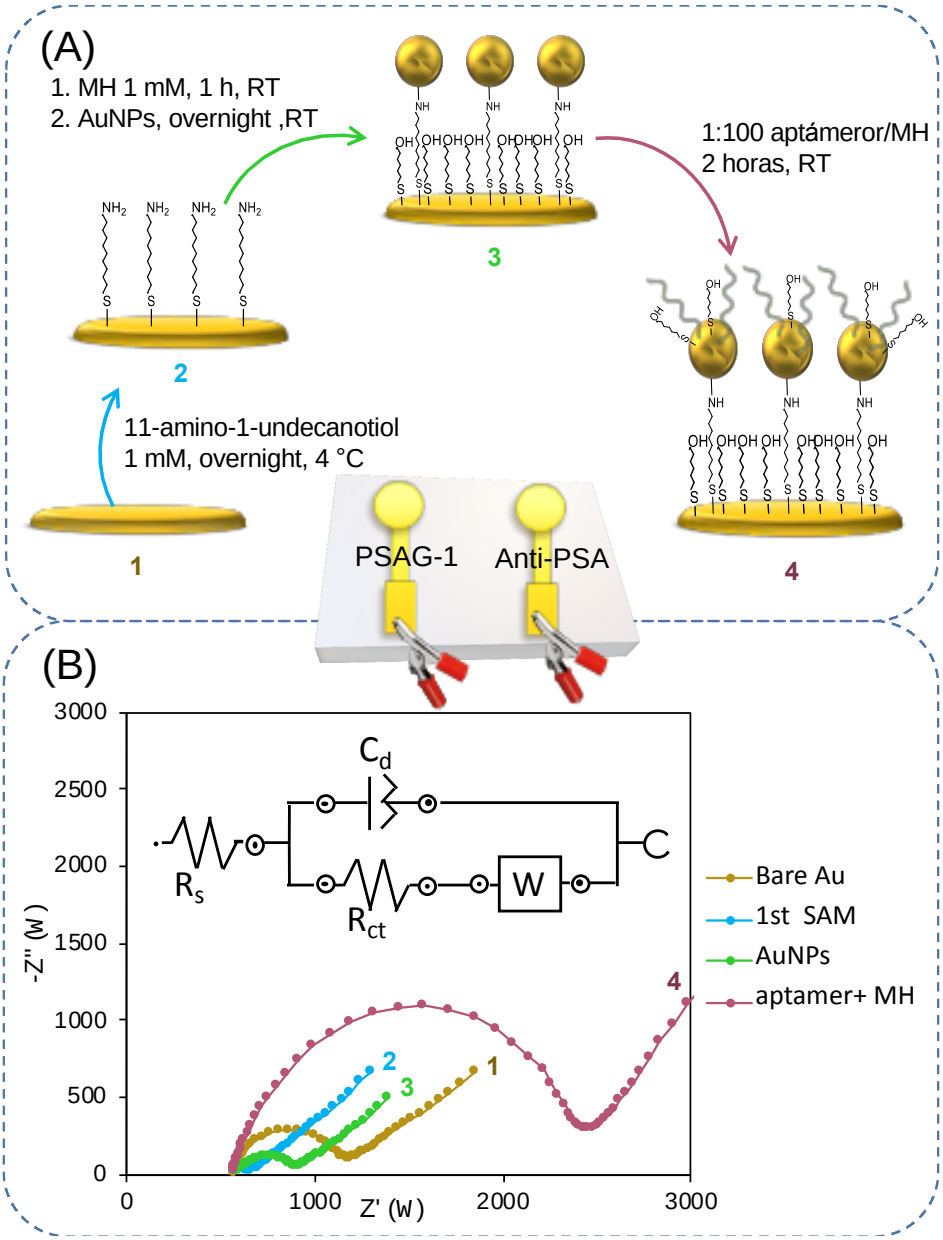

Figure 1. A) Steps involved in the construction of the dual impedimetric aptamer-based platform for the sequential measurement of PSAG-1 reactive PSA and total PSA. B)

Nyquist plot recorded in a PBS solution with 5 mM $[Fe(CN)_6]^{3-/4-}$ during the stepwise aptasensors fabrication. The inset shows the Randles equivalent circuit used to fit the experimental data.

3.1 Characterization of the affinity of the immobilized aptamers.

The first step in the design of the dual-impedimetric platform is the identification of the appropriate aptamers that achieve clinically relevant affinity and selectivity towards different regions of PSA. The selected aptamers have shown ability to bind to immobilized human PSA (hPSA), a glycosylated form of the protein, although with different affinities i.e. dissociation constants (K_d) of 177 ± 5 nM for anti-PSA (Díaz-Fernández et al., 2019), and 1.9 ± 0.2 nM for PSAG-1 (Díaz-Fernández et al., 2020) as estimated by SPR measurements with the aptamers in solution. In addition, anti-PSA showed even improved affinity (K_d = 70 ± 5 nM) (Díaz-Fernández et al., 2019) towards recombinant PSA (rPSA), an unglycosylated form of the protein. These results suggest that anti-PSA recognizes PSA by a region different from the glycosylation site, while the fucose-core plays an important role in the formation of the PSAG-1:hPSA complex (Díaz-Fernández et al., 2020). However, previous studies have indicated that the interaction aptamer-protein depends on which partner has been immobilized due to surface interactions (Amaya-González et al., 2015; Daniel et al., 2013; Miranda-Castro et al., 2018). The immobilization of the aptamers onto the sensing surface could change their conformation and their ability to bind to the protein. Consequently, the adopted configuration for the design of the impedimetric platform could modify the aptamer affinity binding due to changes in the aptamer accessibility or steric hindrance between near aptamers (Daniel et al., 2013). Consistent with this, we tested in the proposed configuration (immobilized aptamer and protein in solution) the affinities of both aptamers towards hPSA. To evaluate this, we immobilized the

thiolated aptamers onto SPR gold chips establishing a refractive angle baseline in the PBS buffer solution, followed by titration with increasing concentrations of hPSA. Fitting the titration curves to the Langmuir model, which assumes a 1:1 stoichiometry, yielded a dissociation constant of 223 ± 65 nM for PSAG-1 and 336 ± 63 nM for anti-PSA (**Figure 2**). It is therefore apparent that in the proposed configuration (immobilized aptamer and protein in solution) both aptamers showed a decrease in their affinities towards hPSA.

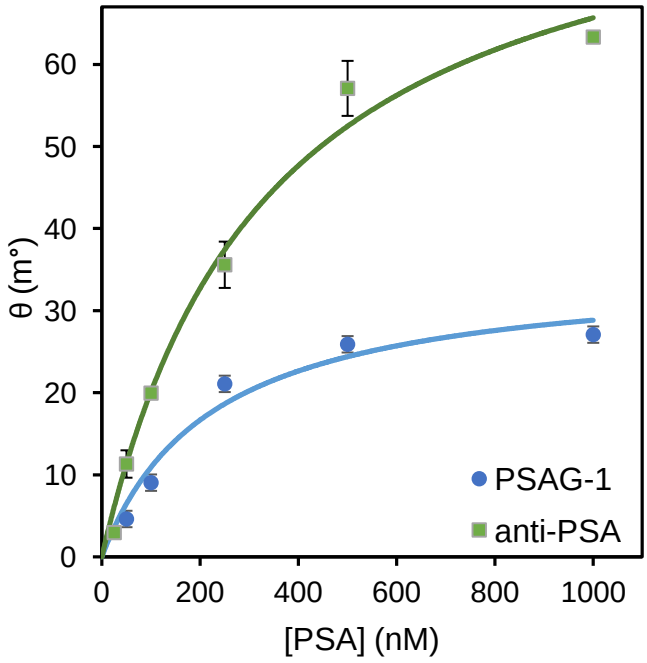

Figure 2. SPR binding curves obtained after incubation of the SPR-chip modified with each aptamer: anti-PSA (green square) and PSAG-1 (blue circles) with increasing amounts of hPSA. Solid lines represent the fit to the Langmuir model.

Although the immobilization of the aptamers, with the corresponding conformational constrains, leads to a reduction in their affinity towards the protein, the magnitude of this effect is different in both cases. While the affinity of anti-PSA diminished by two-fold, that of PSAG-1 decreased by more than 100 times. There are two potentially significant differences. First, both aptamers recognize different epitopes

on the protein, with different accessibility. Second, the hPSA standard used for titration may contain different glycosylation forms, and it has been previously found that about 77% of the standard PSA isolated from seminal fluid carries core-fucosylated N-glycans (Llop et al., 2016). Nevertheless, the obtained affinities support PSA measurements across the clinical range.

3.2 Analytical performance of the impedimetric aptamer-based platform.

To obtain information about the fraction of hPSA that is reactive to the aptamer PSAG-1, the two adjacent sensing surfaces in the designed platform, one modified with the aptamer PSAG-1 and the second one with anti-PSA, were challenged with increasing concentrations of hPSA in PBS. The binding of the protein produced an increase in the R_{ct} value, obtained from the Nyquist plot. To correct variations due to the differences in the microscopic surface area of the sensing phase and in the aptamer-packing, we used as read-out signal the percent change in R_{ct} with respect to the initial value, in the absence of protein, $R_{ct,0}$. In both cases, this signal increases with increasing hPSA concentrations until it approaches saturation (**Figure 3A & 3B**). We found that PSAG-1 aptasensor leads to higher signals than the anti-PSA one. At saturating hPSA level the sensing phase fabricated with PSAG-1 exhibited 39.7 ± 0.5 % of R_{ct} increase, while the anti-PSA sensor gave a 26.5 ± 0.9 % change. This difference is higher at low hPSA concentrations, for example at 0.64 ng/mL of hPSA the response of PSAG-1 sensor is 2.7 times that of anti-PSA. Consequently, the dynamic range of the response covers from 0.64 ng/mL to 62.5 ng/mL for anti-PSA aptamer, and 0.26 ng/mL to 62.5 ng/mL for PSAG-1 aptamer. This probably stems from two effects: the differences in the affinity constant of the two aptamers and the different orientation of the protein once bound to the sensing phase taking into account that both aptamers recognize different epitopes in the protein.

The PSAG-1-sensing phase, in contrast, produces a much smaller signal increase for rPSA, while the surface modified with anti-PSA gives rise to similar signal changes for hPSA and rPSA (**Figure 3A & 3B**). The signal increase for anti-PSA when we employ rPSA is 96% of that of hPSA versus only 37 % when using PSAG-1 as receptor. This again confirms the differences in the recognition site of both aptamers, being PSAG-1 the only one that recognizes the glycosylation site of the protein.

As a demonstration of the selectivity of our platform, we next challenged it with human serum albumin (HSA), the most abundant protein in human serum. After incubation of both aptasensors with 10 ng/mL of HSA in PBS for 30 min, we find that the percentage of change in the R_{ct} (0.4 ± 0.3 % for the PSAG-1 sensor and 2.9 ± 0.5 % for anti-PSA) was significantly lower than the obtained for the same concentration of hPSA (36 ± 2 % in the case of PSAG-1 and 21.0 ± 0.5 % for anti-PSA).

The sensors also support effective hPSA sensing in serum samples. One of the most important challenges to overcome when working in this complex medium is to minimize the non-specific adsorption of other components of the matrix. To minimize these effects, we diluted the serum 5-fold with PBS buffer and conditioned the sensing phase by incubating it for 30 min in women serum, with a PSA content <0.01 ng/mL certified by an ELISA test. We used the R_{ct} value obtained after this conditioning step as reference. The signal increase we observed under these conditions for increasing concentrations of hPSA is similar to that seen in buffer within the low concentration range (**Figure 3A & 3B**). For example, at 0.64 ng/mL of hPSA the PSAG-1 sensing phase leads to a 7.6 ± 0.4 % of increase in diluted serum (*vs.* 7.4 ± 0.2 % of change in buffer). In consequence, the useful dynamic range in serum is the same as in buffer. However, the saturating signals are lower than that seen in buffer, probably because the

number of recognition sites is reduced due to the adsorption of other proteins present in the serum matrix during the conditioning.

The calibration curves obtained in diluted serum were fitted to Langmuir equation $y = (y_{max} \cdot x)/(P + x)$, where y_{max} is the saturation response and P the concentration leading to 50% of the maximum signal, with a y_{max} value of 27.2 ± 0.8 % and P of 4.8 ± 0.5 ng/mL with a correlation of 0.996 for anti-PSA aptamer (Figure 3B), and a y_{max} value of 36 ± 2 % and P of 2.3 ± 0.4 ng/mL with a correlation of 0.993 for PSAG-1 aptamer (**Figure 3A**).

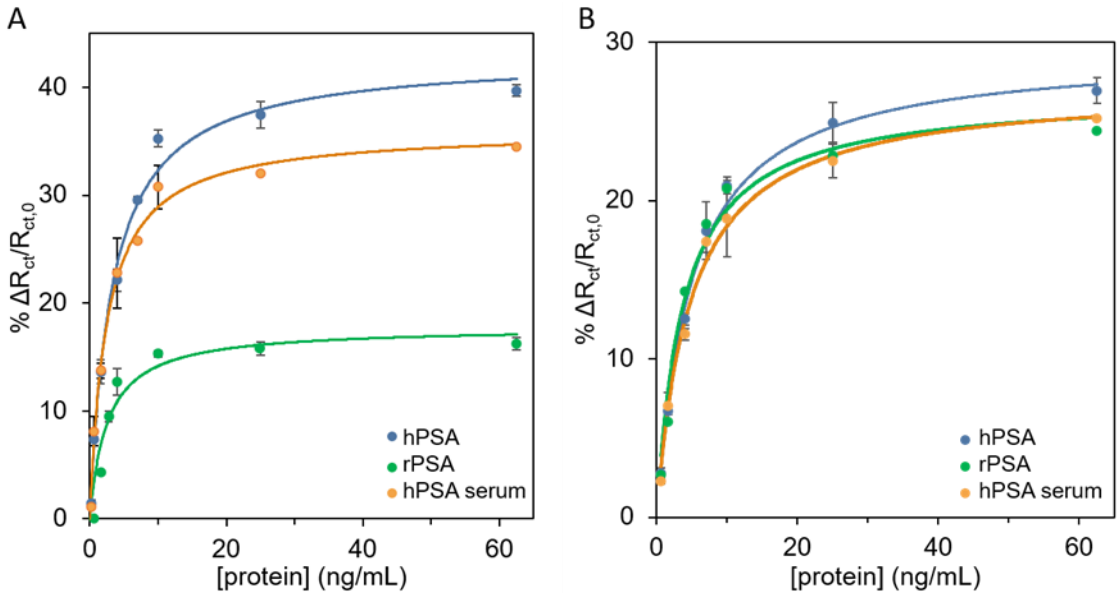

Figure 3. Calibration curve for the dual impedimetric platform. The PSAG-1 (A) and the anti-PSA (B) sensing interfaces respond efficiently to hPSA in PBS (blue circles) and in 5-fold diluted serum (orange circles). PSAG-1 sensor shows a much smaller response to rPSA (green circles) than anti-PSA sensor. The lines represent fits of the data to a Langmuir equation. Error bars represent the standard deviation of measurements with three independently fabricated sensors.

3.3 Analysis of PSA in clinical samples

To explore the clinical utility of our platform we next challenged it for detecting PCa associated PSA glycan alterations. Hospital Universitario de Cabueñes (Gijón-Asturias) provided us serum samples from 12 patients classified in three groups: patients with a benign prostate pathology, with diagnosed PCa, and healthy (see Table 1). The samples were selected with levels of total PSA in the grey zone or above (> 4 ng/mL), quantified with the automated ADVIA Centaur® (Siemens) ELISA assay at the central laboratory of the hospital.

The impedimetric platform first conditioned in free-PSA serum was incubated with the 5-fold diluted serum sample. The percentage of change in R_{ct} obtained with each sensor was referred to the corresponding calibration curve in diluted serum to obtain the concentration of PSA. We observed that the results obtained with the anti-PSA-modified sensing phase perfectly matched those obtained in the hospital with the commercial ELISA (**Figure 4A**). On the other hand, the PSAG-1 based sensor gives concentration values consistently lower than those obtained with the anti-PSA sensor. This is in agreement with the fact that PSAG-1 reactive PSA represents only a fraction of total PSA in the sample.

To evaluate the diagnostic value of the proposed dual-approach we defined the glycan score (GS) as the ratio between the concentration measure with PSAG-1 aptamer and the concentration measure with anti-PSA aptamer (total PSA) multiplied by 100. Neither total PSA nor PSAG-1 reactive PSA clearly correlates with the state of health of the patient (see specific values in Table 1 and Box-and-Whisker plots in the Supplementary Information Figures S1 and S2). On the contrary, GS significantly correlates with the final diagnosis (Table 1, **Figures 4B** and S3), distinguishing non-PCa patients from patients finally diagnosed with PCa. On the basis of the GS value it is possible to differentiate two groups. The first one with GS values between 22 and 37 for

non PCa patients, includes healthy patients and patients with a benign prostatic illness (prostatitis or benign prostate hyperplasia, BPH). The other group, with GS values between 82 and 86, corresponds to PCa patients. These results are in agreement with a significant increase of PSAG1-reactive PSA in PCa patients, which could be associated to changes in the core-fucosylation levels (Li et al., 2015) or an increase in highly branched glycan structures associated to cancer (Munkley et al., 2016). The glycan score could be a good alternative for the diagnosis of PCa in men with levels of PSA in the grey zone or above, with potential to improve the clinical outcomes of PSA test and to reduce the number of unnecessary biopsies.

Table 1: Levels of total and glycosylated PSA of each sample and value of the glycan score.

Sample	[tPSA] (ng/mL)	[gPSA] (ng/mL)	Glycan score	Diagnosis
1	9.2 ± 0.2	2.6 ± 0.5	28 ± 5	Diabetes type II (DMII), hypertension
2	5.6 ± 0.3	1.22 ± 0.01	22 ± 1	DMII
3	9.1 ± 0.4	2.7 ± 0.2	29 ± 2	aortic prosthesis
4	8 ± 1	1.83 ± 0.08	24 ± 3	morbid obesity
5	12.7 ± 0.3	10 ± 1	82 ± 9	Prostate cancer
6	42 ± 2	35 ± 2	83 ± 6	Prostate cancer
7	5.6 ± 0.6	4.8 ± 0.1	86 ± 10	Prostate cancer
8	10.4 ± 0.2	8.8 ± 0.4	84 ± 3	Prostate cancer
9	5.48	2.0 ± 0.8	37 ± 13	prostatitis
10	7.6 ± 0.9	2.6 ± 0.5	30 ± 6	Prostate cancer
11	29 ± 1	8.8 ± 0.4	30 ± 2	BPH
12	92.6	25 ± 2	27 ± 2	BPH

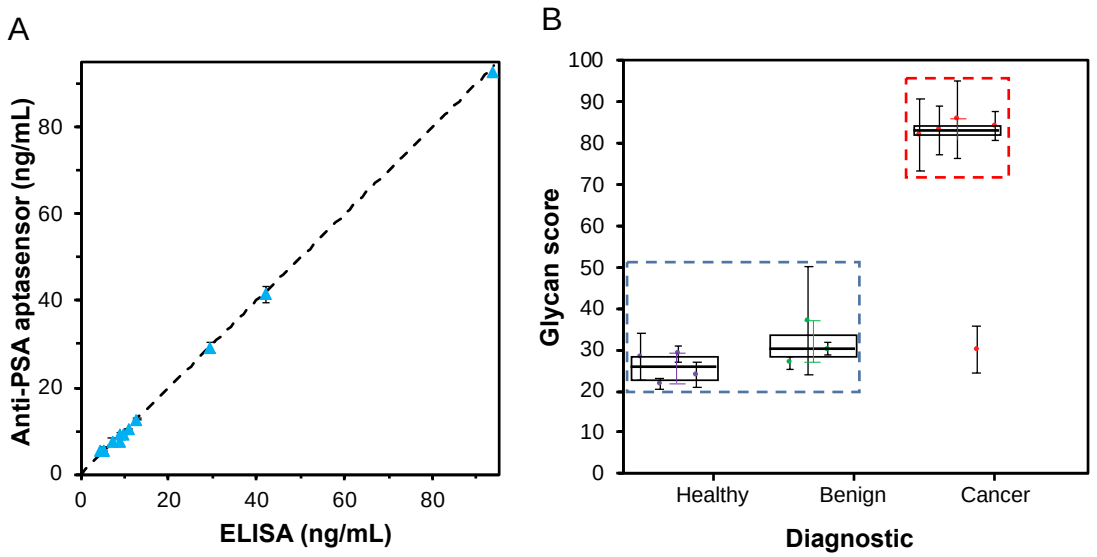

Figure 4. Results of the analysis of serum samples with the impedimetric dual-platform. A) Correlation between total PSA serum levels found by a standard ELISA and those obtained with the anti-PSA aptamer-based sensor. B) Correlation between the glycan score, obtained as the ratio between PSAG-1 reactive PSA and total PSA, and the diagnosed pathology.

4. Conclusions

The finding that prostate tumour malignancy is associated with changes in the glycosylation pattern of PSA motivates the development of a new liquid biopsy test for PCa diagnostic. The availability of the aptamer PSAG-1 to recognize the core-glycan and the surrounding peptide in PSA opens the door to the development of new diagnostic tests for improving the predictive and prognostic value of this biomarker. Here, we demonstrated that a label-free impedimetric platform, which combines PSAG-1 aptamer for directly entrapping specific glycosylated forms of the protein with another aptamer able to bind total PSA, has the potential to achieve this unmet clinical need. The dual system can rapidly and conveniently measure the different fractions of PSA in serum after a simple dilution of the sample. The two sensors have a useful dynamic

range covering the clinical range, with a lower limit of 0.26 ng/mL for the PSAG-1 reactive PSA and 0.64 ng/mL for total PSA and up to 62.5 ng/mL, achieving a reproducibility of 5.4 % across this range. The two signals obtained as read-out of this dual platform are used to calculate the ratio of PSAG-1-reactive PSA to total PSA. This ratio, defined as glycan score, has better predictive power to separate PCa from non-PCa patients than just total PSA. Although further validation is required, our results support the use of the glycan score to reduce unnecessary biopsies without compromising the ability to diagnose PCa.

CRediT authorship contribution statement

Ana Díaz-Fernández: Methodology, Investigation, Data curation, Writing - original draft, Writing - review & editing. **Rebeca Miranda-Castro**: Data curation, Methodology, Writing - review & editing. **Noemí de-los-Santos Álvarez**: Conceptualization, Data curation, Methodology, Writing - review & editing. **María Jesús Lobo-Castañón:** Conceptualization, Resources, Project administration, Supervision, Writing - review & editing. **Pedro Estrela**: Conceptualization, Resources, Supervision, Writing - review & editing.

Declaration of competing interest

The authors declare no competing financial interest.

Acknowledgments

We thank Dr. E. Fernández-Rodríguez and Dr. S. García-Alonso (Hospital Universitario de Cabueñes-Asturias) for providing the serum samples. The work was funded by the Spanish Ministerio de Ciencia y Universidades (RTI-2018-095756-B-I00), and Principado de Asturias Government (IDI2018-000217), co-financed by FEDER funds. A.D.F. was supported by Asociación Española contra el Cáncer (AECC) with a Ph.D. fellowship and by Banco Santander and University of Oviedo with a grant in the framework of the economic mobility of excellence grants for teachers and researchers.

References

Akiba, U., Anzai, J., 2016. Recent progress in electrochemical biosensors for glycoproteins. Sensors 16, 2045. https://doi.org/10.3390/s16122045

Amaya-González, S., López-López, L., Miranda-Castro, R., de-los-Santos-Álvarez, N., Miranda-Ordieres, A.J., Lobo-Castañón, M.J., 2015. Affinity of aptamers binding 33-mer gliadin peptide and gluten proteins: Influence of immobilization and labeling tags. Anal. Chim. Acta 873, 63–70. https://doi.org/10.1016/j.aca.2015.02.053

Butler, E.N., Kelly, S.P., Coupland, V.H., Rosenberg, P.S., Cook, M.B., 2020. Fatal prostate cancer incidence trends in the United States and England by race, stage, and treatment. Br. J. Cancer 123, 487–494. https://doi.org/10.1038/s41416-020-0859-x

Catalona, W.J., Partin, A.W., Sanda, M.G., Wei, J.T., Klee, G.G., Bangma, C.H., Slawin, K.M., Marks, L.S., Loeb, S., Broyles, D.L., Shin, S.S., Cruz, A.B., Chan, D.W., Sokoll, L.J., Roberts, W.L., Van Schaik, R.H.N., Mizrahi, I.A., 2011. A multicenter study of [-2]pro-prostate specific antigen combined with prostate specific antigen and free prostate specific antigen for prostate cancer detection in the 2.0 to 10.0 ng/ml prostate specific antigen range. J. Urol. 185, 1650–1655. https://doi.org/10.1016/j.juro.2010.12.032

Damborska, D., Bertok, T., Dosekova, E., Holazova, A., Lorencova, L., Kasak, P., Tkac, J., 2017. Nanomaterial-based biosensors for detection of prostate specific antigen. Microchim. Acta 184, 3049–3067. https://doi.org/10.1007/s00604-017-2410-1

Daniel, C., Roupioz, Y., Gasparutto, D., Livache, T., Buhot, A., 2013. Solution-Phase vs Surface-Phase aptamer-protein affinity from a label-free kinetic biosensor. PLoS One 8, e75419. https://doi.org/10.1371/journal.pone.0075419

Díaz-Fernández, A., Miranda-Castro, R., de-los-Santos-Álvarez, N., Fernández-Rodríguez, E., Lobo-Castañón, M.J., 2019. Focusing aptamer selection on the glycan structure of prostate-specific antigen: Toward more specific detection of prostate cancer. Biosens. Bioelectron. 128, 83–90. https://doi.org/10.1016/j.bios.2018.12.040

Díaz-Fernández, A., Miranda-Castro, R., Díaz, N., Suárez, D., de-los-Santos-Álvarez, N., Lobo-Castañón, M.J., 2020. Aptamers targeting protein-specific glycosylation in tumor biomarkers: general selection, characterization and structural modeling. Chem. Sci. https://doi.org/10.1039/d0sc00209g

Ghorbani, F., Abbaszadeh, H., Dolatabadi, J.E.N., Aghebati-Maleki, L., Yousefi, M., 2019. Application of various optical and electrochemical aptasensors for detection of human prostate specific antigen: A review. Biosens. Bioelectron. 142. https://doi.org/10.1016/j.bios.2019.111484

Gilgunn, S., Conroy, P.J., Saldova, R., Rudd, P.M., O'Kennedy, R.J., 2013. Aberrant PSA glycosylation - A sweet predictor of prostate cancer. Nat. Rev. Urol. 10, 99–107. https://doi.org/10.1038/nrurol.2012.258

Jeong, S., Han, S.R., Lee, Y.J., Lee, S.W., 2010. Selection of RNA aptamers specific to active prostate-specific antigen. Biotechnol. Lett. 32, 379–385. https://doi.org/10.1007/s10529-009-0168-1

Jolly, P., Damborsky, P., Madaboosi, N., Soares, R.R.G., Chu, V., Conde, J.P., Katrlik, J., Estrela, P., 2016. DNA aptamer-based sandwich microfluidic assays for dual quantification and multi-glycan profiling of cancer biomarkers. Biosens. Bioelectron. 79, 313–319. https://doi.org/10.1016/J.BIOS.2015.12.058

Jolly, P., Zhurauski, P., Hammond, J.L., Miodek, A., Liébana, S., Bertok, T., Tkáč, J., Estrela, P., 2017. Self-assembled gold nanoparticles for impedimetric and

amperometric detection of a prostate cancer biomarker. Sensors Actuators B Chem. 251, 637–643. https://doi.org/10.1016/J.SNB.2017.05.040

Jung, M., Xu, C., Spethmann, J., Johannsen, M., Deger, S., Stephan, C., Loening, S.A., Jung, K., 2004. DD3PCA3-based molecular urine analysis for the diagnosis of prostate cancer. Eur. Urol. 46, 271–273. https://doi.org/10.1016/j.eururo.2004.03.003

Li, M., Guo, X., Li, H., Zuo, X., Hao, R., Song, H., Aldalbahi, A., Ge, Z., Li, J., Li, Q., Song, S., Li, S., Shao, N., Fan, C., Wang, L., 2018. Epitope binning assay using an electron transfer-modulated aptamer sensor. ACS Appl. Mater. Interfaces 10, 341–349. https://doi.org/10.1021/acsami.7b17324

Li, Q.K., Chen, L., Ao, M.H., Chiu, J.H., Zhang, Z., Zhang, H., Chan, D.W., 2015. Serum fucosylated prostate-specific antigen (PSA) improves the differentiation of aggressive from non-aggressive prostate cancers. Theranostics 5, 267–276. https://doi.org/10.7150/thno.10349

Llop, E., Ferrer-Batallé, M., Barrabés, S., Guerrero, P.E., Ramírez, M., Saldova, R., Rudd, P.M., Aleixandre, R.N., Comet, J., de Llorens, R., Peracaula, R., 2016. Improvement of prostate cancer diagnosis by detecting PSA glycosylation-specific changes. Theranostics 6, 1190–1204. https://doi.org/10.7150/thno.15226

Lomas, D.J., Ahmed, H.U., 2020. All change in the prostate cancer diagnostic pathway. Nat. Rev. Clin. Oncol. 17, 372–318. https://doi.org/10.1038/s41571-020-0332-z

Macefield, R., Metcalfe, C., Lane, J., Donovan, J., Avery, K., Blazeby, J., Down, L., Neal, D., Hamdy, F., Vedhara, K., 2010. Impact of prostate cancer testing: an evaluation of the emotional consequences of a negative biopsy result. Br. J. Cancer 102, 1335–1340. https://doi.org/10.1038/sj.bjc.6605648

Miranda-Castro, R., de-los-Santos-Álvarez, N., Lobo-Castañón, M.J., 2018.

Characterization of aptamer-ligand complexes, in: Aptamers for Analytical Applications. Wiley-VCH Verlag GmbH & Co. KGaA, Weinheim, Germany, pp. 127–172. https://doi.org/10.1002/9783527806799.ch4

Munkley, J., Mills, I.G., Elliott, D.J., 2016. The role of glycans in the development and progression of prostate cancer. Nat. Rev. Urol. 13, 324–333. https://doi.org/10.1038/nrurol.2016.65

Negahdary, M., Sattarahmady, N., Heli, H., 2020. Advances in prostate specific antigen biosensors-impact of nanotechnology. Clin. Chim. Acta 504, 43–55. https://doi.org/10.1016/j.cca.2020.01.028

Park, J.W., Lee, S.J., Ren, S., Lee, S., Kim, S., Laurell, T., 2016. Acousto-microfluidics for screening of ssDNA aptamer. Sci. Rep. 6. https://doi.org/10.1038/srep27121

Peracaula, R., Tabarés, G., Royle, L., Harvey, D.J., Dwek, R.A., Rudd, P.M., de Llorens, R., 2003. Altered glycosylation pattern allows the distinction between prostate-specific antigen (PSA) from normal and tumor origins. Glycobiology 13, 457–470. https://doi.org/10.1093/glycob/cwg041

Pihíková, D., Belicky, S., Kasák, P., Bertok, T., Tkac, J., 2016a. Sensitive detection and glycoprofiling of a prostate specific antigen using impedimetric assays. Analyst 141, 1044–1051. https://doi.org/10.1039/c5an02322j

Pihíková, D., Kasak, P., Kubanikova, P., Sokol, R., Tkac, J., 2016b. Aberrant sialylation of a prostate-specific antigen: Electrochemical label-free glycoprofiling in prostate cancer serum samples. Anal. Chim. Acta 934, 72–79. https://doi.org/10.1016/j.aca.2016.06.043

Saini, S., 2016. PSA and beyond: alternative prostate cancer biomarkers. Cell. Oncol. 39, 97–106. https://doi.org/10.1007/s13402-016-0268-6

Savory, N., Abe, K., Sode, K., Ikebukuro, K., 2010. Selection of DNA aptamer against

prostate specific antigen using a genetic algorithm and application to sensing. Biosens. Bioelectron. https://doi.org/10.1016/j.bios.2010.07.057

Schröder, F.H., Hugosson, J., Roobol, M.J., Tammela, T.L.J., Ciatto, S., Nelen, V., Kwiatkowski, M., Lujan, M., Lilja, H., Zappa, M., Denis, L.J., Recker, F., Berenguer, A., Määttänen, L., Bangma, C.H., Aus, G., Villers, A., Rebillard, X., van der Kwast, T., Blijenberg, B.G., Moss, S.M., de Koning, H.J., Auvinen, A., 2009. Screening and prostate-cancer mortality in a randomized european study. N. Engl. J. Med. 360, 1320–1328. https://doi.org/10.1056/NEJMoa0810084

Song, E., Hu, Y., Hussein, A., Yu, C.Y., Tang, H., Mechref, Y., 2015. Characterization of the glycosylation site of human PSA prompted by missense mutation using LC-MS/MS. J. Proteome Res. 14, 2872–2883. https://doi.org/10.1021/acs.jproteome.5b00362

Srivastava, M., Nirala, N.R., Srivastava, S.K., Prakash, R, 2018. A comparative Study of Aptasensor Vs Immunosensor for Label-Free PSA Cancer Detection on GQDs-AuNRs Modified Screen-Printed Electrodes. Sci. Rep. 8, 1923. https://doi.org/10.1038/s41598-018-19733-z

Svobodova, M., Bunka, D.H.J., Nadal, P., Stockley, P.G., O'Sullivan, C.K., 2013. Selection of 2′F-modified RNA aptamers against prostate-specific antigen and their evaluation for diagnostic and therapeutic applications. Anal. Bioanal. Chem. 405, 9149–9157. https://doi.org/10.1007/s00216-013-7350-y

Xia, N., Cheng, C., Liu, L., Peng, P., Liu, C., Chen, J., 2017. Electrochemical glycoprotein aptasensors based on the in-situ aggregation of silver nanoparticles induced by 4-mercaptophenylboronic acid. Microchim. Acta 184, 4393–4400. https://doi.org/10.1007/s00604-017-2488-5

CRediT authorship contribution statement

Ana Díaz-Fernández: Methodology, Investigation, Data curation, Writing - original draft, Writing - review & editing. **Rebeca Miranda-Castro**: Data curation, Methodology, Writing - review & editing. **Noemí de-los-Santos Álvarez**: Conceptualization, Data curation, Methodology, Writing - review & editing. **María Jesús Lobo-Castañón:** Conceptualization, Resources, Project administration, Supervision, Writing - review & editing. **Pedro Estrela**: Conceptualization, Resources, Supervision, Writing - review & editing.

Supplementary Information

Impedimetric Aptamer-based Glycan PSA Score better Discriminates Prostate Cancer from other Prostate Diseases

Ana Díaz-Fernández[1,2], Rebeca Miranda-Castro[1,2], Noemí de-los-Santos-Álvarez[1,2], María Jesús Lobo-Castañón[1,2]* and Pedro Estrela[3,4]*.

[1] Departamento de Química Física y Analítica. Universidad de Oviedo, Av. Julián Clavería 8, 33006 Oviedo, Spain.

[2] Instituto de Investigación Sanitaria del Principado de Asturias, Avenida de Roma, 33011 Oviedo, Spain.

[3] Centre for Biosensors, Bioelectronics and Biodevices (C3Bio), University of Bath, BA2 7AY, Bath, United Kingdom.

[4] Department of Electronic and Electrical Engineering, University of Bath, BA2 7AY, Bath, United Kingdom.

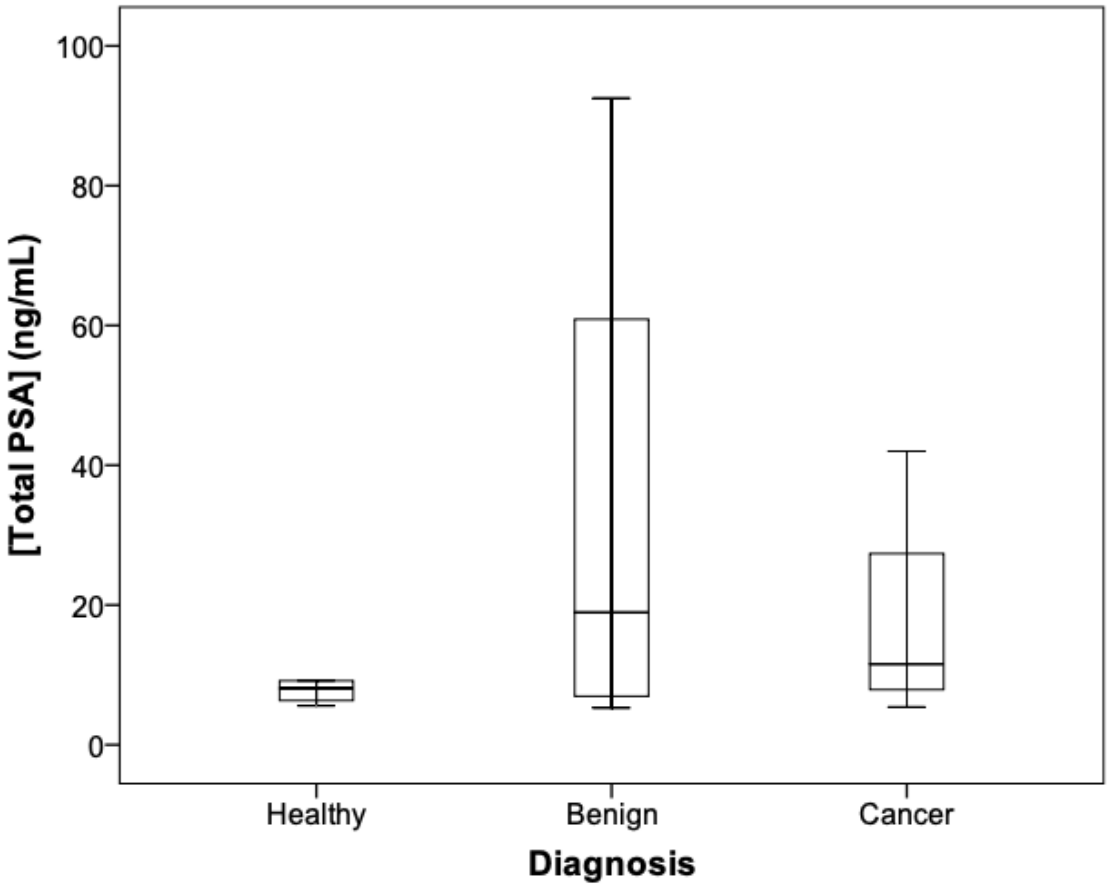

Figure S1: Box-and-Whisker plot for total PSA concentration, measured with the anti-PSA impedimetric sensor, in serum of patients with different diagnosis of prostate pathologies.

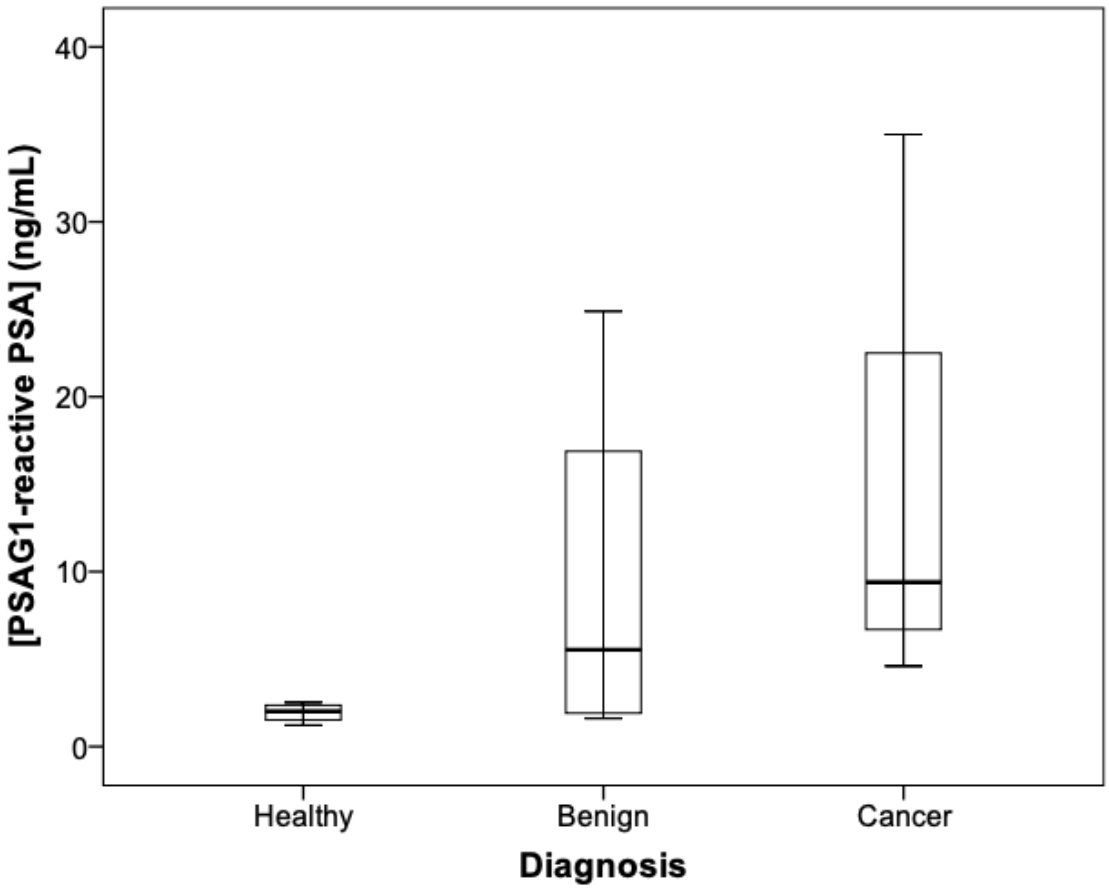

Figure S2: Box-and-Whisker plot of PSAG-1 reactive PSA concentration, measured with the PSAG-1 impedimetric sensor, in serum of patients with different diagnosis of prostate pathologies.

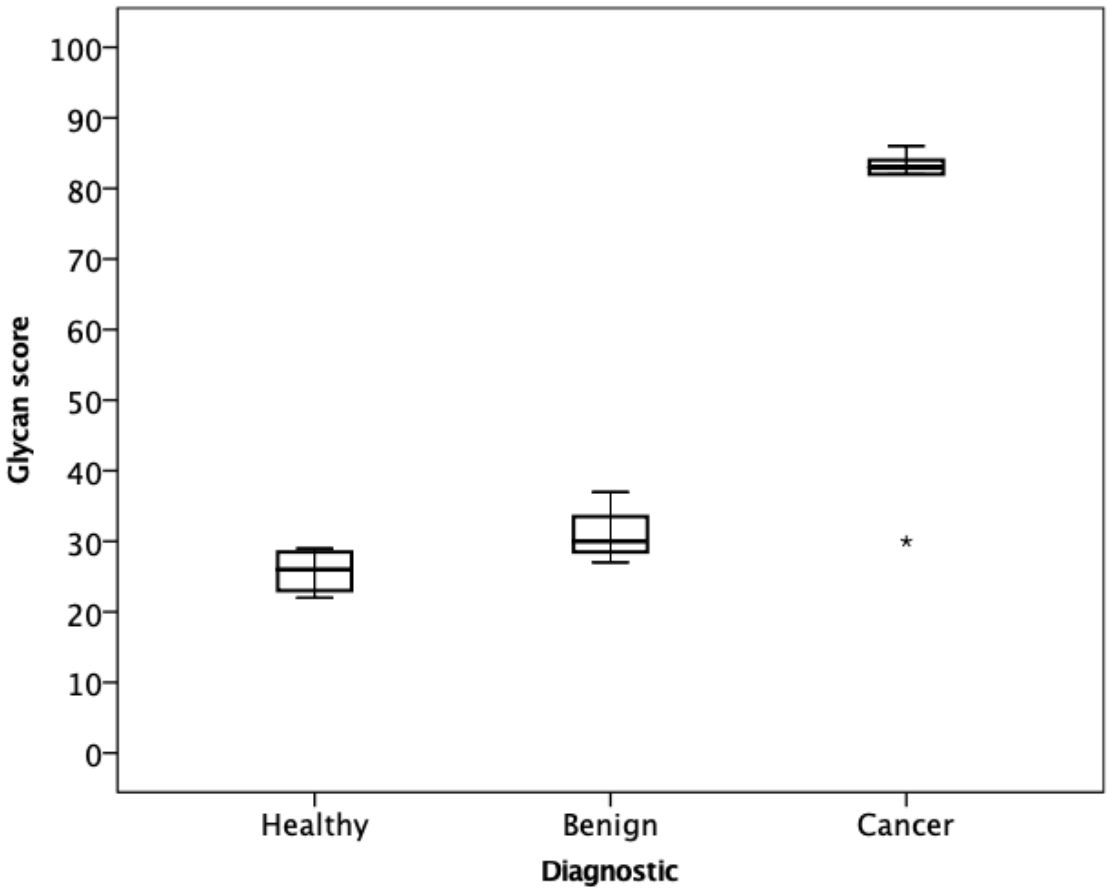

Figure S3: Box-and-Whisker plot for the glycan score (PSAG-1 reactive PSA / total PSA × 100) obtained in serum of patients with different diagnosis of prostate pathologies.